Supporting Information

The non-planarity of the Benzene Molecule in the X-ray Structure of the Chelated Bismuth(III) Heteroboroxine Complex Is not Supported by Quantum Mechanical Calculations

Jindřich Fanfrlík,[a] Robert Sedlak,[a] Adam Pecina,[a] Lubomír Rulíšek,[a] Libor Dostál,[b] Ján Moncóľ,[c] Aleš Růžička,*[b] and Pavel Hobza*[a,d]

[a] *Institute of Organic Chemistry and Biochemistry, Academy of Sciences of the Czech Republic, 166 10 Prague 6, Czech Republic. Email: hobza@uochb.cas.cz*

[b] *Department of General and Inorganic Chemistry, Faculty of Chemical Technology, University of Pardubice, Studentská 573, CZ-532 10, Pardubice, Czech Republic. Email: ales.ruzicka@upce.cz*

[c] *Institute of Inorganic Chemistry, Faculty of Chemical and Food Technology, Slovak University of Technology, Slovak University of Technology, SK-812 37 Bratislava, Slovakia*

[d] *Regional Centre of Advanced Technologies and Materials, Department of Physical Chemistry, Palacký University, 771 46 Olomouc, Czech Republic.*

TABLE OF CONTENTS:

Calculations

Using the X-ray crystal structure of the chelated bismuth(III) heteroboroxine complex, we have modeled the distorted benzene molecule. We considered the central benzene molecule with its surroundings, i.e. two whole chelated bismuth(III) heteroboroxine complexes and four fragments (two benzene and two propane molecules). The obtained model (Figure S1) has 252 atoms and was described at the DFT-D3/TPSS/TZVPP level of theory using Turbomole 6.6{1} and Cuby3.{2} All the hydrogen atoms were optimized in the first step. In the second step, all the atoms of the central benzene molecule were optimized. In order to investigate the potential energy surface (PES) of the benzene molecule within the complex, we used a relaxed scan. The benzene molecule was moving between the two Bi atoms in two ways. First, center of mass of benzene was constrained. Second, only the single C atom was constrained. In the both cases, the relaxed scans were performed, i.e. all other atoms of the benzene molecule were optimized (remaining heavy atoms of the complex were kept rigid). Finally, the relaxed scan with the singe C atom constrained was also recalculated using B-P86, PBE and B97D functionals.

For the interaction energy decomposition (SAPT method), electrostatic potential (ESP) electron differential maps calculations, we used a smaller model where 2,6-diisopropylphenyls were not considered (the model shown in Figure 5). A hybrid DFT-SAPT{4} method was used here for decomposition of the total interaction energies using a gradient-controlled shift procedure at PBE0/aug-cc-pVDZ and PBE0/TZVP level. Electrostatic, induction and exchange-repulsion terms were evaluated at PBE0/aug-cc-pVDZ level and dispersion energies were calculated empirically. Bromine, Iodine and Bismuth atoms were treated by pseudopotentials to describe relativistic effects of inner-core electrons correctly and the frozen core approximation was used to speed the calculations up.

ESP of the whole chelated bismuth(III) heteroboroxine complex on 0.001 a.u. was computed at the B97D/def2-QZVP level using Gaussian09.{3}

Electron differential maps were also calculated at the B97D/def2-QZVP level of theory. However, the isodensity of 0.00033 a.u. (1/3 of the 0.001 a.u. isodensity value) was depicted. The cubegen utility was used to generate cube files. All the electron density images were created via MOLEKEL 4.3 program.

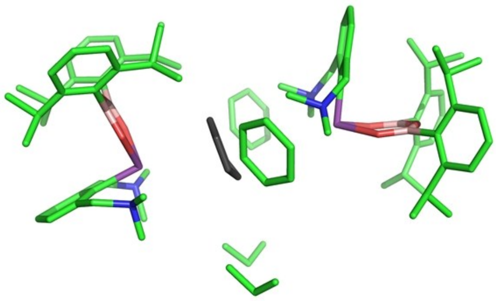

Figure S1. The model used for DFT-D3/TPSS/TZVPP calculations. The color coding is as follows: carbon atoms of the central benzene molecule, gray; carbon, green; bismuth, violet; oxygen, red; ping, boron; nitrogen, blue.

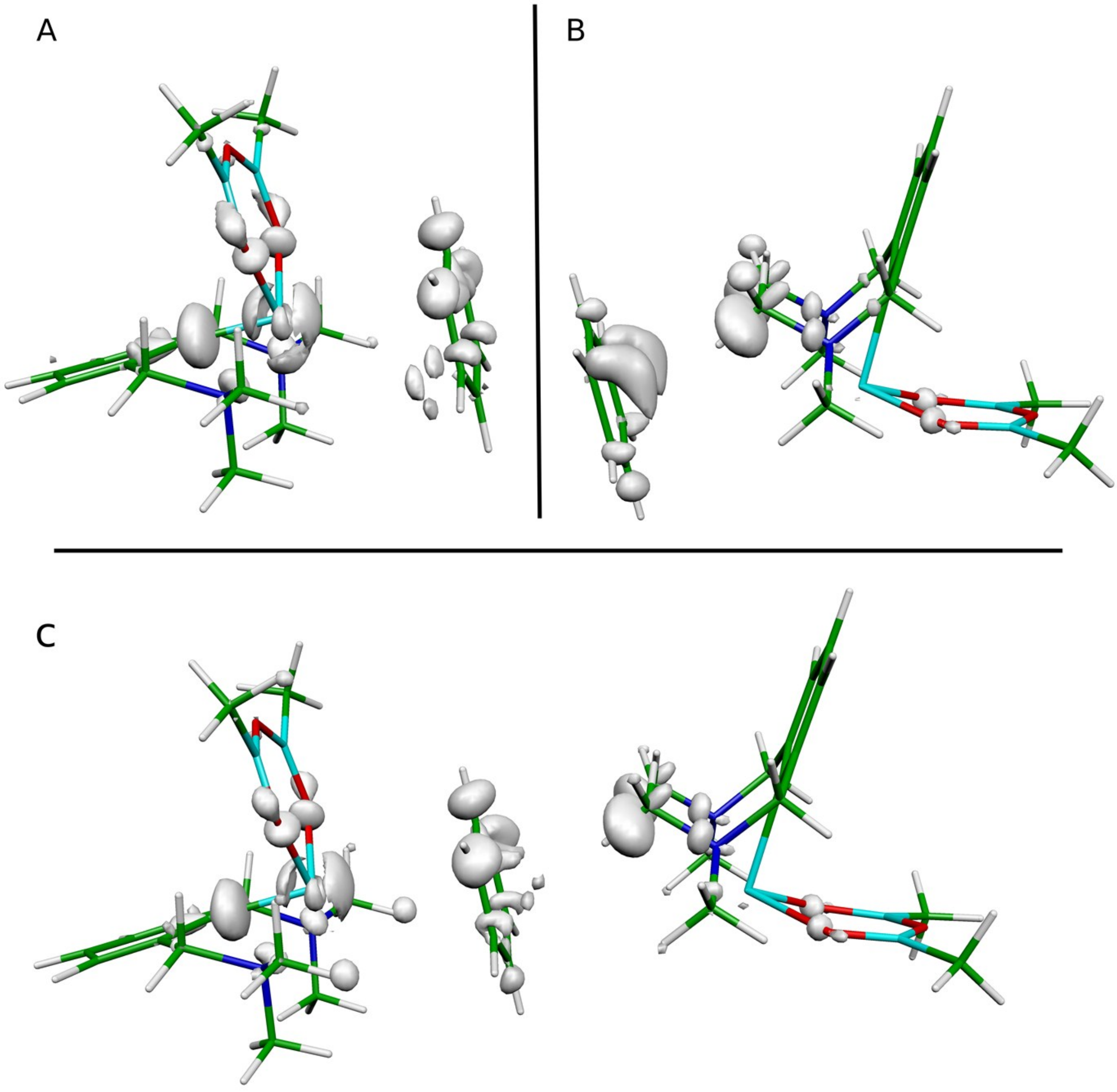

Figure S2. Electron differential map of the Bi...benzene...Bi complex. The 0.00033 a.u. isodensity surface is depicted; for the binary Bi(1)···benzene complex (A), the binary benzene···Bi(2) complex (B) and the tertiary Bi(1)···benzene···Bi(2) adduct (C).

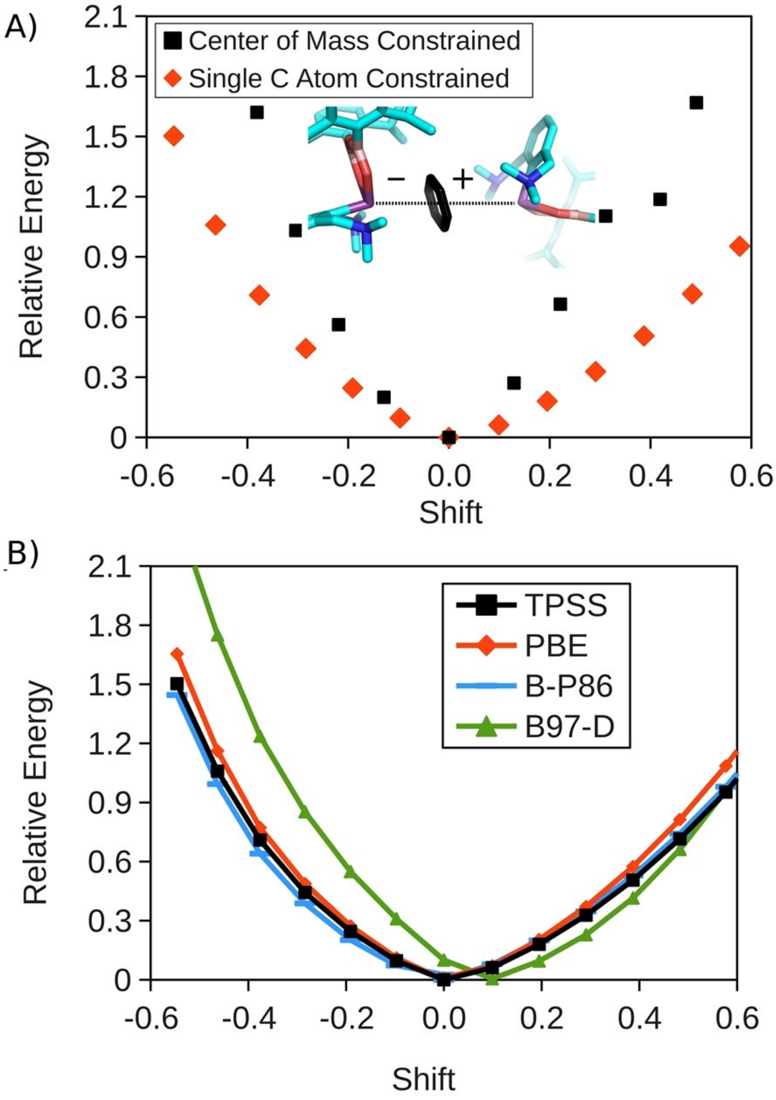

Figure S3. A) Relative energy (in kcal/mol) at the DFT-D3/TPSS/TZVPP level obtained by the relaxed scan plotted against shift of the benzene molecule (in Å). The benzene molecule was moving between the two Bi atoms in two ways. First, center of mass of benzene was constrained. Second,, only the single C atom was constrained. In the both cases, the relaxed scans were performed, i.e. all other atoms of the benzene molecule were optimized (remaining heavy atoms of the complex were kept rigid). B) The relaxed scan with the single C atom constrained recalculated by using PBE, B-P86 and B97-D functionals.

Crystallography

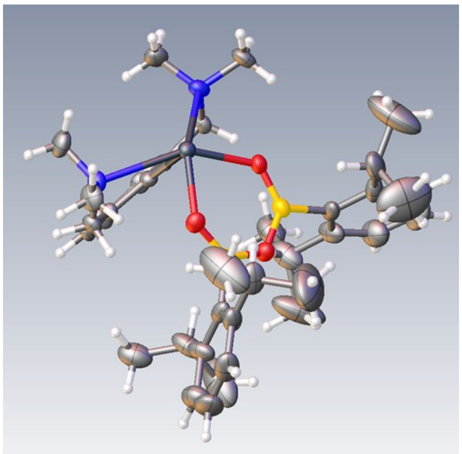

Fig. S4 ORTEP view of organobismuth heteroboroxine - benzene complex. One of the independent parts of the complex is shown only, the second disordered part and the solvent molecules (benzene - masked by the SQUEEZE program) are omitted for clarity.

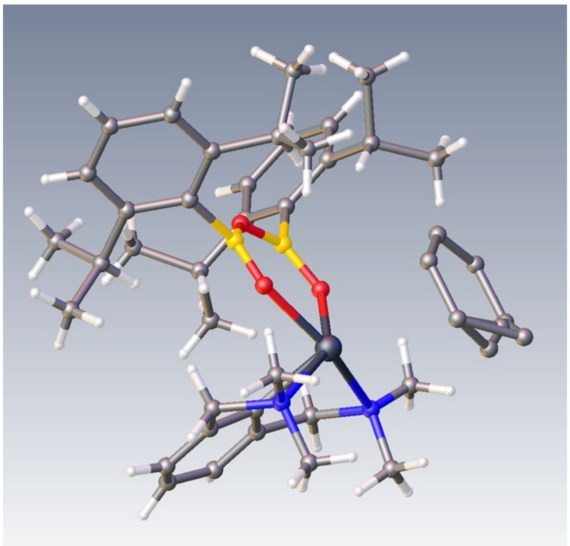

Fig. S5 Diagram of organobismuth heteroboroxine - benzene complex. One of the independent parts of the complex is shown only - primary refinement showing the el. maxima found in the area of benzene ring as carbon atoms.

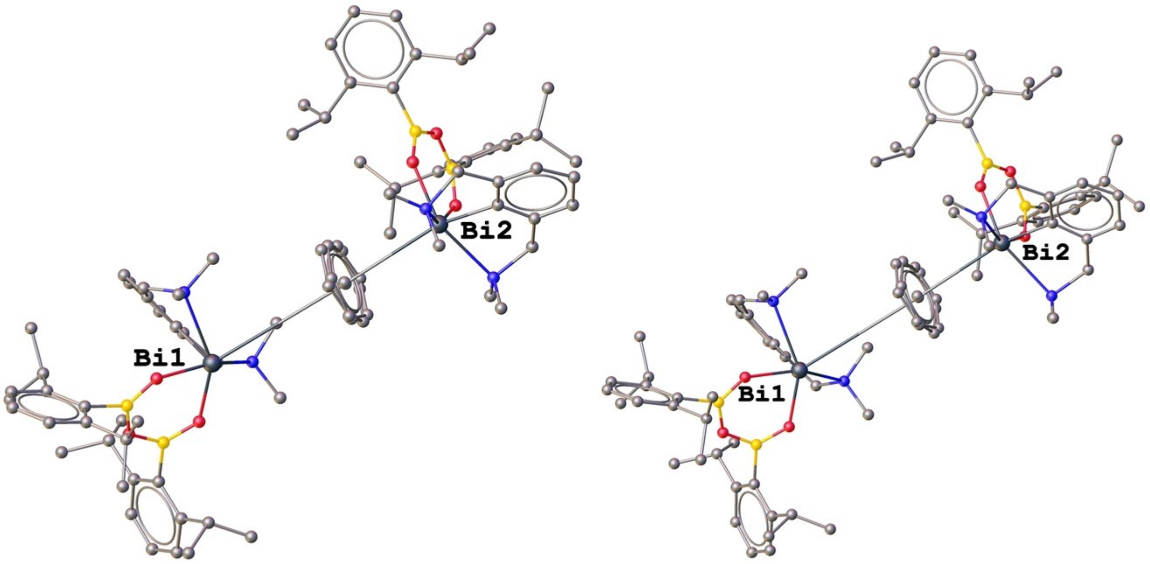

Fig. S6 ORTEP view of organobismuth heteroboroxine - benzene complex-different treatment. Independent interacting parts of the complex are shown only, the disordered part of the ligand and the solvent molecule (non-interacting benzene) are omitted for clarity. Final treatment with SHELXT, SHELXL-2014/7, WinGX-2014.1, SQUEEZE programs.

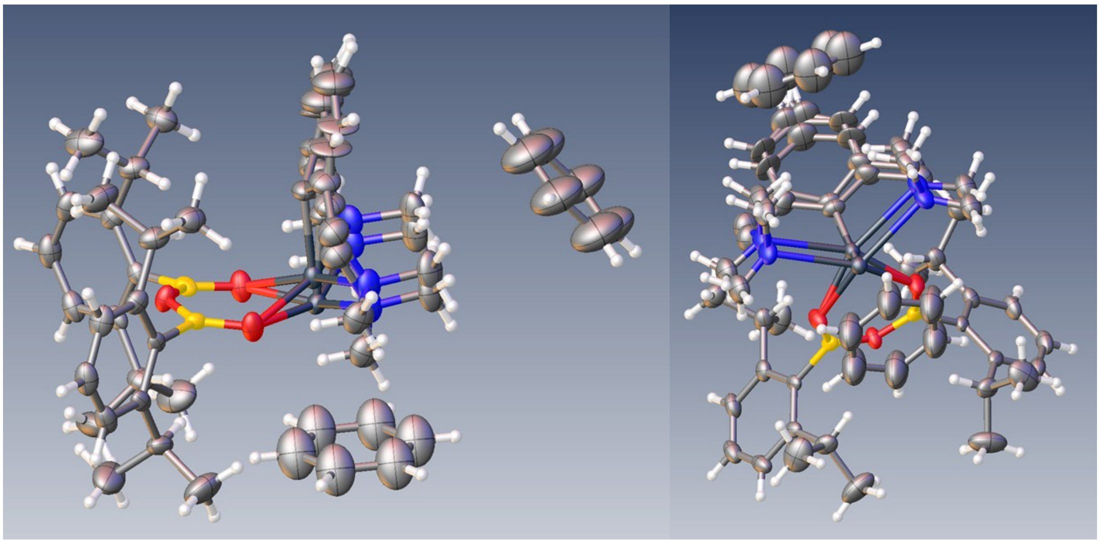

Fig. S7 ORTEP view of organobismuth heteroboroxine - benzene complex - top and side view. One of the independent parts (disordered part) of the complex is shown only - a superposition of benzene, the second part and the solvent molecule (benzene) are omitted for clarity. Final treatment with SHELXT, SHELXL-2014/7, WinGX-2014.1, SQUEEZE programs.

Procedures, parameters

The X-ray data for colorless crystals of organobismuth heteroboroxine - benzene complex (six different crystals from three different crystallization crops) were obtained at 100, 150 and 200 K using Oxford Cryostream low-temperature device on a Nonius KappaCCD diffractometer with Mo Kα radiation ($\lambda = 0.71073$ Å), a graphite monochromator, and the ϕ and χ scan mode. Data reductions were performed with DENZO-SMN[5]. The absorption was corrected by integration methods[6]. All structures were primarily solved by direct methods (Sir92)[7] and refined by full matrix leastsquares based on F^2 (SHELXL97)[8] giving almost the same results. Hydrogen atoms were mostly localized on a difference Fourier map, however to ensure uniformity of treatment of crystal, all hydrogen were recalculated into idealized positions (riding model) and assigned temperature factors Hiso(H) =1.2Ueq(pivot atom) or of 1.5Ueq for the methyl moiety with C-H = 0.96, 0.97, 0.98 and 0.93 Å for methyl, methylene, methine and hydrogen atoms in aromatic ring, respectively.

The final structure with superimposed/disordered benzene molecules, refined disorder of one of the ligands and Bi atoms and masked residual electron density was obtained by treatment of selected dataset by SHELXT, SHELXL-2014/7[9], WinGX-2014.1[10], SQUEEZE[11] programs.

There is residual electron density probably originated from a disordered solvent (benzene) in the structure of organobismuth heteroboroxine - benzene complex. Attempts were made to model this disorder or split it into two positions, but were unsuccessful. PLATON/SQUEZZE[11] was used to correct the data for the presence of disordered solvent. A potential solvent volume of 629 Å^3 was found. 142 electrons per unit cell worth of scattering were located in voids. The calculated stoichiometry of solvent was calculated to be four molecules of benzene per unit cell which results in 168 electrons per unit cell. CCDC Nr. 1414464.

Table S1: Crystallographic data for organobismuth heteroboroxine - benzene complex - refinement performed by SHELXT, SHELXL-2014/7, WinGX-2014.1, SQUEEZE programs.

empirical formula	$C_{36}H_{53}B_2BiN_2O_3$ (C_6H_6)
crystal system	tetragonal
space group	$P4_2/m$
a[Å]	21.483(2)
b[Å]	21.4830(18)
c[Å]	19.0040(10)
β[°]	90
Z	8
μ[mm^{-1}]	4.056
D_x [Mg m^{-3}]	1.315
cryst size [mm]	0.33 x 0.22 x 0.21
θ range, [deg]	4.165- 26.37
T_{min}, T_{max}	0.403, 0.533
no. of reflns measd	43816
no. of unique reflns, $R_{\mathrm{int}}{}^a$	9046, 0.0541
no. of obsd reflns [$I>2\sigma(I)$]	6525
no. of params	438
S^b all data	1.124
final R^c indices [$I>2\sigma(I)$]	0.0499
wR^{2c} indices (all data)	0.0875
Δρ, max., min. [e Å^{-3}]	1.466, -1.092

^{a} $R_{\mathrm{int}} = \Sigma|F_o^2 - F_{o,\mathrm{mean}}^2|/\Sigma F_o^2$, ^{b} $S = [\Sigma(w(F_o^2 - F_c^2)^2)/(N_{\mathrm{diffrs}} - N_{\mathrm{params}})]^{½}$. $^c R(F) = \Sigma||F_o| - |F_c||/\Sigma|F_o|$, $wR(F^2) = [\Sigma(w(F_o^2 - F_c^2)^2)/(\Sigma w(F_o^2)^2)]^{½}$.

References

1 R. Ahlrichs, M. Bar, M. Haser, H. Horn and C. Kolmel, *Chem. Phys. Lett.,* 1989, **162**, 165.

2 J. Rezac, Cuby 3, Prague.

3 Gaussian 09, Revision D.01, M. J. Frisch, G. W. Trucks, H. B. Schlegel, G. E. Scuseria, M. A. Robb, J. R. Cheeseman, G. Scalmani, V. Barone, B. Mennucci, G. A. Petersson, H. Nakatsuji, M. Caricato, X. Li, H. P. Hratchian, A. F. Izmaylov, J. Bloino, G. Zheng, J. L. Sonnenberg, M. Hada, M. Ehara, K. Toyota, R. Fukuda, J. Hasegawa, M. Ishida, T. Nakajima, Y. Honda, O. Kitao, H. Nakai, T. Vreven, J. A. Montgomery, Jr., J. E. Peralta, F. Ogliaro, M. Bearpark, J. J. Heyd, E. Brothers, K. N. Kudin, V. N. Staroverov, R. Kobayashi, J. Normand, K. Raghavachari, A. Rendell, J. C. Burant, S. S. Iyengar, J. Tomasi, M. Cossi, N. Rega, J. M. Millam, M. Klene, J. E. Knox, J. B. Cross, V. Bakken, C. Adamo, J. Jaramillo, R. Gomperts, R. E. Stratmann, O. Yazyev, A. J. Austin, R. Cammi, C. Pomelli, J. W. Ochterski, R. L. Martin, K. Morokuma, V. G. Zakrzewski, G. A. Voth, P. Salvador, J. J. Dannenberg, S. Dapprich, A. D. Daniels, Ö. Farkas, J. B. Foresman, J. V. Ortiz, J. Cioslowski, and D. J. Fox, Gaussian, Inc., Wallingford CT, 2009.

4 A. Hesselmann, *J. Phys. Chem. A*, 2011, **115**, 11321.

5 Z. Otwinowski and W. Minor, *Methods in Enzymology* 1997, **276**, 307.

6 P. Coppens In: F.R. Ahmed, S.R. Hall and C.P. Huber Editors, Crystallographic Computing, **1970**, pp. 255 – 270, Copenhagen, Munksgaard.

7 A. Altomare, G. Cascarano, C. Giacovazzo and A. Guagliardi, *Journal of Applied Crystallography* 1994, **27**, 1045.

8 G. M. Sheldrick, SHELXL-97, University of Göttingen: Göttingen, **2008**.

9 G. M. Sheldrick, *Acta Cryst.* 2015, C**71**, 3.

10 L. J. Farrugia, *J. Appl. Cryst.* 2012, **45**, 849.

11 P. van der Sluis, and A. L. Spek, *Acta Crystalllogr.,* 1990, **A46**, 194.